Arabian Journal of Chemistry (2016) 9, S1218–S1224

King Saud University

Arabian Journal of Chemistry

www.ksu.edu.sa
www.sciencedirect.com

ORIGINAL ARTICLE

# Investigation of the effect of piperidin-1-yl-phosphonic acid on corrosion of iron in sulfuric acid

M.R. laamari [a,*], J. Benzakour [a], F. Berrekhis [b], M. Bakasse [c], D. Villemin [d]

[a] *Laboratoire Physico-Chimie des Matériaux et Environnement, Université Cadi Ayyad, Faculté des Sciences Semlalia, BP 2390 Marrakech, Morocco*
[b] *Laboratoire de Chimie Physique, Ecole Normale Supérieure, BP 2400 Marrakech, Morocco*
[c] *Laboratoire de Chimie Organique, Biorganique et Environnement, Université Chouaib Doukkali, Faculté des Sciences, El Jadida, Morocco*
[d] *École Nationale Supérieure d'Ingénieurs de Caen UMR 6507 CNRS, Bd Maréchal Juin 14050, Caen Cedex, France*

Received 8 August 2011; accepted 31 January 2012
Available online 15 February 2012

**KEYWORDS**

Iron;
Thermodynamic parameters;
Phosphonic acid;
Inhibition

**Abstract** The inhibitive effect of the piperidin-1-yl-phosphonic acid (PPA) on the corrosion of iron in 1 M $H_2SO_4$ solution has been investigated by weight loss measurement, potentiodynamic polarization and electrochemical impedance spectroscopy (EIS) techniques. The presence of (PPA) reduces remarkably the corrosion rate of iron in acidic solution. The effect of temperature on the corrosion behavior of iron was studied in the range of 298–328 K. Results clearly reveal that the (PPA) behaves as a mixed type corrosion inhibitor with the highest inhibition at $5 \times 10^{-3}$ M. The adsorption of PPA on the iron surface obeys the Langmuir's adsorption isotherm.
© 2012 Production and hosting by Elsevier B.V. on behalf of King Saud University. This is an open access article under the CC BY-NC-ND license (http://creativecommons.org/licenses/by-nc-nd/3.0/).

## 1. Introduction

Corrosion inhibition as a protective method is of great importance. Inhibitors often work by adsorbing themselves on the metallic surface, protecting it by forming a film. The strength of the adsorption bond is the dominant factor for organic inhibitors. Their effectiveness depends on the chemical composition, their chemical structure and their affinity for the metal surface. A wide variety of compounds are used as corrosion inhibitors for metals in acidic media (Schmitt, 1984; Mernari et al., 1998; Onuchukwu, 1988; Ashassi-Sorkhabi and Nabavi-Amri, 2000; Ebenso, 2002; Gomma, 1998; Ayers and Hackerman, 1963; Szauer and Brandt, 1981; Morad, 2008).

Phosphonates, which were originally introduced as scale inhibitors in water treatment, were later proved to be good corrosion inhibitors also (Awad and Turgoose, 2004). Their impact on the environment was reported to be negligible at the concentration levels used for corrosion inhibition (Awad, 2005; Jaworska et al., 2002). There are excellent sequestering agents for electroplating, chemical plating, degreasing and cleaning (Fang et al., 1993). The use of phosphonic acids for the protection of iron and its alloys from corrosion in different media has been the subject of several research works (Choi et al., 2002; Gonzalez et al., 1996; Ebenso, 2002; Telegdi

* Corresponding author. Fax: +212 5 24 62 70 26.
E-mail address: r.laamari@ucam.ac.ma (M.R. laamari).
Peer review under responsibility of King Saud University.

Production and hosting by Elsevier

http://dx.doi.org/10.1016/j.arabjc.2012.01.013
1878-5352 © 2012 Production and hosting by Elsevier B.V. on behalf of King Saud University.
This is an open access article under the CC BY-NC-ND license (http://creativecommons.org/licenses/by-nc-nd/3.0/).

et al., 2001; Amar et al., 2003, 2008; Laamari et al., 2001, 2004, 2010, 2011a, 2016).

In this work we continue our investigations on piperidin-1-yl-phosphonic acid as inhibitors of Armco iron corrosion mainly in 1 M $H_2SO_4$. The assessment of the corrosion behavior was studied using weight loss, potentiodynamic polarization measurement and electrochemical impedance spectroscopy (EIS). Thermodynamic data were also obtained from adsorption isotherms and Arrhenius plots.

## 2. Experimental

### 2.1. Electrochemical cell

Electrochemical experiments were performed using a conventional three electrode cell assembly. The working electrode is a carbon steel rotating disk with a surface area of 1 $cm^2$ and had the following composition (O: 0.03%, Mn: 0.03%, N: 0.018%, S: 0.018%, C: 0.012%, P: 0.004%, Fe: 99.8%). It is abraded with different emery papers up to 1200 grade, washed thoroughly with double-distilled water, degreased with AR grade ethanol, acetone, and subjected to drying at room temperature.

A saturated calomel electrode (SCE) was used as the reference electrode. All the measured potentials presented in this paper are referred to this electrode. The counter electrode was a platinum plate with a surface area of 2 $cm^2$.

The aggressive solution of 1.0 M $H_2SO_4$ was prepared by the dilution of AR grade 98% $H_2SO_4$ with distilled water. The inhibitor is added to freshly prepared 1 M $H_2SO_4$ in the concentration range of $10^{-4}$ to $5\times10^{-3}$ M.

The corrosion inhibitor used in this work is piperidin-1-yl-phosphonic acid (PPA). The organic compound is synthesized by the micro-wave technique. The obtained product is purified and characterized by $^1$H NMR, $^{13}$C NMR, $^{31}$P NMR spectroscopy and IR techniques. The molecular structure is shown in Fig. 1.

### 2.2. Methods

#### 2.2.1. Gravimetric measurements

Gravimetric measurements were carried out in a double walled glass cell equipped with a thermostat-cooling condenser. The solution volume was 100 mL of 1 M $H_2SO_4$ with and without the addition of different concentrations of inhibitor. The iron specimens used have a rectangular form ($2\times2\times0.05$ cm). The immersion time for the weight loss was 24 h at 298 K and 6 h at other temperatures. After the corrosion test, the specimens of Armco iron were carefully washed in double-distilled water, dried and then weighed. The rinse removed loose segments of the film of the corroded samples. Triplicate experiments were performed in each case and the mean value of the weight loss is reported. Weight loss allowed us to calculate the mean corrosion rate as expressed in mg $cm^{-2}$ $h^{-1}$. The inhibition efficiency (IE %) was determined by using the following equation:

$$IE\% = \frac{CR_0 - CR}{CR_0}\times 100 \quad (1)$$

where, CR and $CR_0$ are the corrosion rates of carbon steel with and without the inhibitor, respectively.

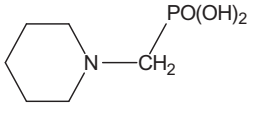


**Figure 1** Structure of piperidin-1-yl-phosphonic acid (PPA).

#### 2.2.2. Electrochemical measurements

Two electrochemical techniques, namely DC-Tafel slope and AC-electrochemical impedance spectroscopy (EIS), were used to study the corrosion behavior. All experiments were performed in one-compartment cell with three electrodes connected to a Voltalab 10 (Radiometer PGZ 100) system controlled by the Volta master 4 corrosion analysis software model.

Polarization curves were obtained by changing the electrode potential automatically from −800 to −200 mV versus open circuit potential ($E_{ocp}$) at a scan rate of 1 $mVs^{-1}$. The inhibition efficiency is calculated by the following equation:

$$IE\% = \frac{i^0_{corr} - i_{corr}}{i^0_{corr}}\times 100 \quad (2)$$

Where $i^0_{corr}$ and $i_{corr}$ are the corrosion current density values without and with the inhibitor, respectively. EIS measurements were carried out under potentiostatic conditions in the frequency range of 100–0.1 Hz, with an amplitude of 10 mV peak-to-peak, using AC signal at $E_{ocp}$. All experiments were performed after immersion for 60 min in 1 M $H_2SO_4$ with and without the addition of inhibitor.

## 3. Results and discussion

### 3.1. Weight loss measurements

#### 3.1.1. Effect of inhibitor concentration

Corrosion inhibition performance of organic compounds as corrosion inhibitors can be evaluated using electrochemical and chemical techniques. For the chemical methods, a weight loss measurement is ideally suited for long term immersion tests. Corroborative results between weight loss and other techniques have been reported (El-Naggar, 2007; Umoren and Ebenso, 2007; El-Etre, 2003; Lebrini et al., 2006).

The anodic dissolution of iron in acidic media and the corresponding cathodic reaction have been reported to proceed as follows (Solomon et al., 2010):

$$Fe \rightarrow Fe^{2+} + 2e- \quad (3)$$

$$2H^+ + 2e- \rightarrow 2H_{ads} \rightarrow H_2 \quad (4)$$

As a result of these reactions, including the high solubility of the corrosion products, the metal loses weight in the solution. The values of corrosion rate and inhibition efficiency from gravimetric measurements at different concentrations of PPT are summarized in Table 1, and the inhibition efficiency as a function of concentration is shown in Fig. 2. The results show that as the inhibitor concentration increases, the corrosion rate decreases and therefore the inhibition efficiency increases. It can be concluded that this inhibitor acts through adsorption on the iron surface and formation of a barrier layer between the metal and the corrosive media. A detailed study on the corrosion behavior of iron was carried out at a temperature range of 298–328 K using the weight loss technique.

**Table 1** Corrosion parameters obtained from weight loss measurements for iron in 1 M $H_2SO_4$ containing various concentrations of PPT at 298 K.

| $C$ (M) | CR (mg cm$^{-2}$ h$^{-1}$) | IE (%) |
|---|---|---|
| Blank | 0.58 | – |
| 0.0005 | 0.23 | 60.34 |
| 0.001 | 0.17 | 70.69 |
| 0.002 | 0.10 | 82.76 |
| 0.004 | 0.05 | 91.38 |

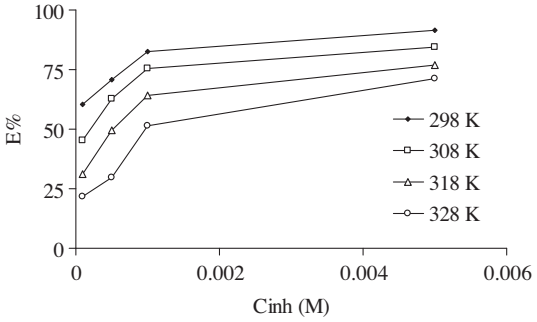


**Figure 2** Variation of inhibition efficiency (IE%) with concentration of PPT for iron in 1 M $H_2SO_4$ at different temperatures.

### 3.1.2. *Effect of temperature*

Temperature has a great effect on the rate of metal electrochemical corrosion. In case of corrosion in an acidic medium the corrosion rate increases exponentially with temperature increase because the hydrogen evolution over potential decreases (Popova et al., 2003). Furthermore, the value of inhibition efficiency indicates the adsorption ability of inhibitor molecules on the metal surface; the higher inhibition efficiency results in the higher adsorption (Shukla and Quraishi, 2009). The effect of temperature on the adsorption behavior of PPT was investigated using weight loss measurements in the temperature range of 298–328 K with and without inhibitor at different concentrations in 1 M $H_2SO_4$. The values of inhibition efficiency obtained are given in Table 2 and Fig. 2. It is clear that inhibition efficiency increased as far as inhibitor concentration increases. The maximum value of inhibition efficiency (IE %) obtained for $5\times10^{-3}$ M PPT is 92% at 298 K. The inhibition efficiencies decrease slightly with increasing temperature, indicating that higher temperature dissolution of iron predominates on adsorption of PPT at the metal surface.

In order to obtain more details on the corrosion process, activation kinetic parameters such as activation energy ($E_a$); enthalpy ($\Delta H°$) and entropy ($\Delta S°$) are obtained from the effect of temperature using Arrhenius law (Eq. (5)) and the alternative formulation of Arrhenius equation (Eq. (6)) (Shukla and Quraishi, 2009; Singh and Quraishi, 2010):

$$\log(\mathrm{CR}) = \log A - \frac{E_a}{2.303RT} \tag{5}$$

$$\mathrm{CR} = \left(\frac{RT}{Nh}\right)\exp\left(\frac{\Delta S^{\circ}}{R}\right)\exp\left(-\frac{\Delta H^{\circ}}{RT}\right) \tag{6}$$

where CR is the corrosion rate, $R$ is the universal gas constant, $T$ is the absolute temperature, $A$ is the pre-exponential factor, $h$ is the Plank's constant ($6.626176\times10^{-34}$ Js) and $N$ is the Avogadro's number ($6.02252\times10^{23}$ mol$^{-1}$).

**Table 2** Corrosion parameters obtained from weight loss for iron in 1 M $H_2SO_4$ containing various concentrations of PPT at different temperatures.

| $C$ (M) | CR (mg cm$^{-2}$ h$^{-1}$) | | | | IE (%) | | | |
|---|---|---|---|---|---|---|---|---|
| | 298 | 308 | 318 | 328 | 298 | 308 | 318 | 328 |
| Blank | 0.58 | 1.02 | 1.70 | 2.5 | – | – | – | – |
| 0.0005 | 0.23 | 0.56 | 1.17 | 1.96 | 60.34 | 45.10 | 31.18 | 21.60 |
| 0.001 | 0.17 | 0.38 | 0.86 | 1.76 | 70.69 | 62.75 | 49.41 | 29.60 |
| 0.002 | 0.10 | 0.25 | 0.61 | 1.22 | 82.76 | 75.49 | 64.12 | 51.20 |
| 0.004 | 0.05 | 0.16 | 0.39 | 0.72 | 91.38 | 84.31 | 77.06 | 71.20 |

The plot of logCR against 1/T for iron corrosion in 1 M $H_2SO_4$ in the absence and presence of different concentrations of PPT is presented in Fig. 3. All parameters are given in Table 3.

In the present study, it could be seen that the activation energy was higher in the presence of inhibitor compared with the blank. In addition, increasing concentration of PPT results in the increasing of the activation energy. Such increase of the activation energies in the presence of inhibitor is attributed to an appreciable decrease in the adsorption process of the inhibitor on the metal surface with increase in temperature; and corresponding increase in the reaction rate because of the greater area of the metal exposed to acid (Abboud et al., 2009). A decrease in inhibition efficiency upon rising the temperature, with analogous increase in corrosion activation energy in the presence of inhibitor compared to its absence, is good evidence for physisorption mechanism of PPT on the iron surface (Abboud et al., 2009; Obot and Obi-Egbedi, 2008, 2010).

Experimental corrosion rate values obtained from weight loss measurements were used to further gain insight on the change of enthalpy ($\Delta H°$) and entropy ($\Delta S°$) of activation for the formation of the activation complex in the transition state using equation (Eq. (6)).

Fig. 4 shows the plot of log (CR/$T$) versus 1/$T$ for iron corrosion in 1 M $H_2SO_4$ in the absence and presence of different concentrations of PPT. Straight lines were obtained with a slope of ($\Delta H°/2.303R$) and an intercept of [log ($R$/Nh)($\Delta S°$/2.303$R$)] from which the values of $\Delta H°$ and $\Delta S°$, respectively were computed and listed also in Table 3. Inspection of these data reveals that the $\Delta H°$ values for dissolution reaction of iron in 1 M $H_2SO_4$ in the presence of PPA are higher (55.82–69.95 kJ mol$^{-1}$) than those of in the absence of inhibitors (40.95 kJ mol$^{-1}$). The positive signs of $\Delta H°$ reflect the endothermic nature of the iron dissolution process suggesting that the dissolution of iron is slow in the presence of inhibitor (Guan et al., 2004). One can notice that $E_a$ and $\Delta H°$ values vary in the same way. This result permits to verify the known thermodynamic reaction between the $E_a$ and $\Delta H°$ as shown in Table 3:

$$\Delta H^{\circ} = E_a - RT \tag{7}$$

On the other hand, $\Delta S°$ increases with increasing PPA concentrations (Table 3) and their values were negative both in the uninhibited and inhibited systems. The negative values of entropies imply that the activated complex in the rate determining step represents an association rather than a

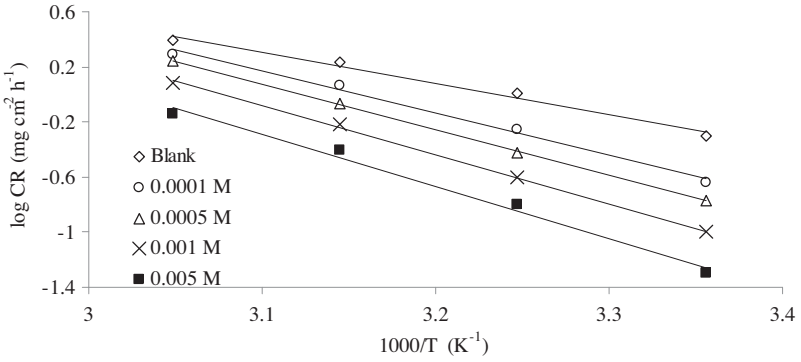


**Figure 3** Arrhenius plots for iron corrosion rates (CR) in 1 M $H_2SO_4$ with and without different concentrations of PPT.

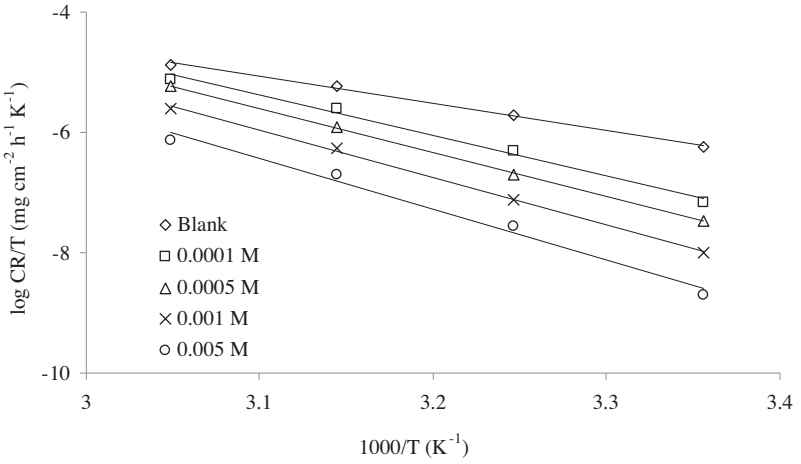


**Figure 4** Transition-state plots for iron corrosion rates (CR) in 1 M $H_2SO_4$ with and without different concentrations of PPT.

**Table 3** Corrosion kinetic parameters for iron in 1 M $H_2SO_4$ with and without different concentrations of PPT.

| $C$ (M) | $E_a$ (kJ mol$^{-1}$) | $R$ | $\Delta H°$ (kJ mol$^{-1}$) | $\Delta S°$ (J mol$^{-1}$) |
|---|---|---|---|---|
| Blank | 43.57 | 0.988 | 37.26 | −135.07 |
| 0.0005 | 58.43 | 0.992 | 55.82 | −80.17 |
| 0.001 | 63.68 | 0.999 | 61.07 | −65.71 |
| 0.002 | 68.36 | 0.998 | 65.75 | −54.14 |
| 0.004 | 72.57 | 0.988 | 69.95 | −45.09 |

dissociation step, meaning that a decrease in disordering takes place ongoing from reactants to the activated complex (Herrag et al., 2010). Moreover, $\Delta S°$ values are more positive in 1 M $H_2SO_4$ solutions containing PPA than those obtained in the uninhibited solution. This behavior can be explained as a result of the replacement process of water molecules during adsorption of PPA on the metal surface (Morad and Kamal El-Dean, 2006). This observation is in agreement with the findings of other workers (Ahamad et al., 2010; Bouklah et al., 2006; Singh and Quraishi, 2010; Noor and Al-Moubaraki, 2009).

### 3.2. Adsorption isotherm

In order to get a better understanding of the electrochemical process on the metal surface, adsorption characteristics are also studied for PPT. This process is closely related to the adsorption of the inhibitor molecules (Hackerman and Sudbury, 1950; Hackerman, 1962; Cheng et al., 2007) and adsorption is known to depend on the chemical structure (Ateya et al., 1984; Akiyama and Nobe, 1970). Adsorption isotherms are very important in determining the mechanism of organic electrochemical reactions. Several adsorption isotherms can be used to assess the adsorption behavior of the inhibitors.

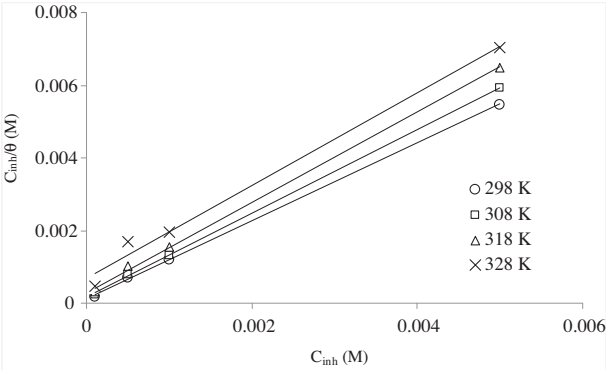


**Figure 5** Langmuir's isotherm adsorption model of PPT on the iron surface in 1 M $H_2SO_4$ at different temperatures.

**Table 4** Thermodynamic parameters for the adsorption of PPT on iron in 1 M $H_2SO_4$ at different temperatures.

| Temperature (K) | $R^2$ | Slope | $K_{ads}$ | $\Delta G^{\circ}_{ads}$ (kJ mol$^{-1}$) |
|---|---|---|---|---|
| 298 | 0.999 | 1.07 | $10^4$ | −32.79 |
| 308 | 0.999 | 1.15 | $5 \times 10^3$ | −32.12 |
| 318 | 0.999 | 1.24 | $3.33 \times 10^3$ | −32.09 |
| 328 | 0.997 | 1.27 | $1.42 \times 10^3$ | −30.79 |

The most frequently used are Langmuir, Temkin and Frumkin. In the hydrochloric acid solution, the organic compound follows the Langmuir adsorption isotherm (Trachli et al., 2002; Li and Mu, 2005; Benabdellah et al., 2011).

According to this isotherm, $\theta$ is related to $C_{inh}$ by:

$$\frac{C_{inh}}{\theta} = \frac{1}{K_{ads}} + C_{inh} \quad (8)$$

where $\theta$ is the surface coverage, $C_{inh}$ is the molar concentration of inhibitor and $K_{ads}$ is the equilibrium constant of the adsorption process.From the values of surface coverage, the linear regressions between $\frac{C_{inh}}{\theta}$ and $C_{inh}$ are calculated and the parameters are listed in Table 4. Fig. 5 shows the relationship between $\frac{C_{inh}}{\theta}$ and $C_{inh}$ at various temperatures. These results show that the linear regression coefficients ($R$) are almost close to 1.000, indicating that the adsorption of inhibitor onto the iron surface agrees to the Langmuir adsorption isotherm.

The equilibrium constants of the adsorption process ($K_{ads}$) decrease upon increasing the temperature values (Table 4). It is well known that $K_{ads}$ indicates the adsorption power of the inhibitor onto the metal surface. Clearly, PPT gives higher values of $K_{ads}$ at lower temperatures, indicating that it was adsorbed strongly onto the iron surface. Thus, the inhibition efficiency decreased slightly with the increase in temperature as the result of the improvement of desorption of PPT from the metal surface.

The standard adsorption free energy ($\Delta G^{\circ}_{ads}$) is obtained according to the following equation:

$$\Delta G^{\circ}_{ads} = -2.303RT\log(55.5K_{ads}) \quad (9)$$

where $R$ is the universal gas constant, $T$ is the thermodynamic temperature, and the value 55.5 is the molar concentration of water in the solution.

The large values of $\Delta G^{\circ}_{ads}$ and its negative sign are usually characteristic of a strong interaction and a high efficient adsorption (Hosseini and Azimi, 2009). Generally, values of $\Delta G_{ads}$ up to −20 kJ mol$^{-1}$ are consistent with physisorption while those around −40 kJ mol$^{-1}$ or higher are associated with chemisorption as a result of sharing or transferring of electrons from organic molecules to the metal surface to form a coordinate type of bond (Obot and Obi-Egbedi, 2008; Bouklah et al.,

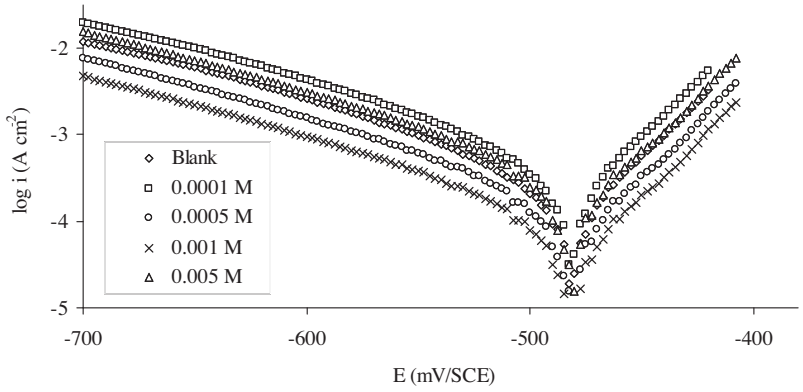


**Figure 6** Potentiodynamic polarization curves for iron in 1 M $H_2SO_4$ containing different concentrations of PPT.

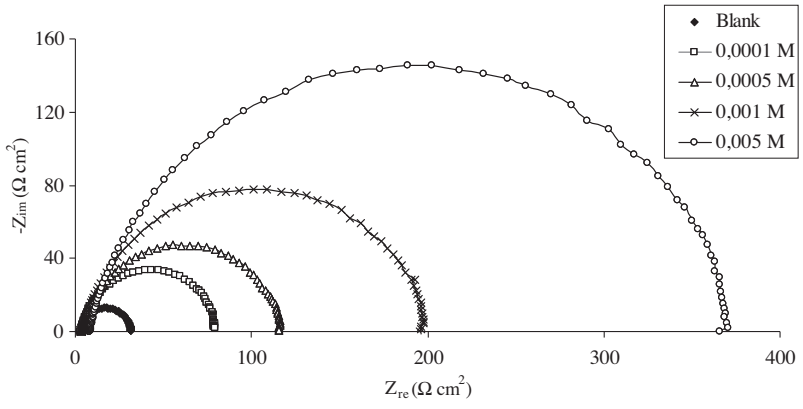


**Figure 7** Nyquist plot for iron in 1 M $H_2SO_4$ with and without different concentrations of PPT.

**Table 5** Polarization parameters and the corresponding inhibition efficiency of iron corrosion in 1 M $H_2SO_4$ containing different concentrations of PPT at 298 K.

| $C$ (M) | $E_{corr}$ (mV/SCE) | $I_{corr}$ (μA $cm^{-2}$) | $B_a$ (mV $dec^{-1}$) | $B_c$ (mV $dec^{-1}$) | IE (%) |
|---|---|---|---|---|---|
| 0 | −485 | 542 | 41.4 | −131 | – |
| $5\times10^{-4}$ | −486 | 202 | 42.4 | −107 | 62.73 |
| $10^{-3}$ | −487 | 145 | 42.3 | −135 | 73.24 |
| $2\times10^{-3}$ | −487 | 80 | 40.5 | −108 | 85.23 |
| $4\times10^{-3}$ | −488 | 41 | 38.7 | −113 | 92.43 |

**Table 6** Electrochemical impedance parameters of iron corrosion in 1 M $H_2SO_4$ containing different concentrations of PPT at 298 K.

| $C$ (M) | Re (ohm $cm^2$) | Cd (μF/$cm^2$) | Rp | IE (%) |
|---|---|---|---|---|
| Blank | 2.12 | 49.11 | 29.10 | – |
| 0.0005 | 3.64 | 35.81 | 76.44 | 61.93 |
| 0.001 | 3.69 | 32.42 | 112.30 | 74.08 |
| 0.002 | 4.84 | 26.16 | 192.12 | 84.85 |
| 0.004 | 4.88 | 14.01 | 358.7 | 91.88 |

2006; Ateya et al., 1984). In the present study, the calculated values of $\Delta G^{\circ}_{ads}$ obtained for PPT range between −30.79 and −32.79 kJ $mol^{-1}$ (Table 4), indicating that the adsorption mechanism of PPT on iron in 1 M $H_2SO_4$ solution at the studied temperatures may be a combination of both physisorption and chemisorption (Ahamad et al., 2010; Singh and Quraishi, 2010; Obot and Obi-Egbedi, 2008, 2010). However, a limited decrease in the absolute value of $\Delta G^{\circ}_{ads}$ with an increase in temperature was observed. This behavior is explained by the fact that the adsorption is somewhat unfavorable with increasing experimental temperature, indicating that physisorption has the major contribution while chemisorption has the minor contribution in the inhibition mechanism (Noor and Al-Moubaraki, 2009).

### 3.3. Potentiodynamic polarization studies

The potentiodynamic polarization behavior of Armco iron in 1 M $H_2SO_4$ with the addition of various concentrations of PPT inhibitor is shown in Fig. 6. The corrosion kinetic parameters such as corrosion potential ($E_{corr}$), corrosion current density ($I_{corr}$), anodic and cathodic Tafel slopes ($B_a$ and $B_c$) were derived from these curves and given in Table 5.

As it is show in Fig. 6 and Table 5, cathodic current–potential curves give rise to parallel Tafel lines indicating that the hydrogen evolution reaction is under activation control and the addition of inhibitor does not modify the mechanism of the proton discharge reaction. The cathodic and anodic current densities decrease with the concentration of PPT. This inhibitor causes change in the anodic and cathodic Tafel slopes and no definite trend was observed in the shift of $E_{corr}$ values in the presence of different concentrations of the inhibitor, suggesting that this compound behaves as a mixed-type inhibitor. Also, data show that the inhibition efficiency increased with increasing the inhibitor concentration to attain 92 at $5\times10^{-3}$ M of PPT. This may be due to the adsorption of PPT on the iron/acid interface (Ahamad et al., 2010).

### 3.4. Electrochemical impedance spectroscopy

Electrochemical impedance measurements were carried out in the frequency range from 100 kHz to 0.01 Hz at the open circuit potential. The Nyquist representations of the impedance of iron in 1 M $H_2SO_4$ with and without the addition of various concentrations of PPT are given in Fig. 7. The existence of a single semi circle showed the single charge transfer process during dissolution which is unaffected by the presence of inhibitor molecules. Deviation of perfect circular shape is often referred to the frequency dispersion of interfacial impedance. This anomalous behavior is generally attributed to the inhomogeneity of the metal surface arising from surface roughness or interfacial phenomena (Shih and Mansfeld, 1989; Martinez and Mansfeld-Hukovic, 2003; Elayyachy et al., 2006).

Corrosion kinetic parameters derived from EIS measurements and inhibition efficiencies are given in Table 6. The charge transfer resistance ($R_{ct}$) and the interfacial double layer capacitance ($C_{dl}$) derived from these curves are given in Table 6. In fact, the addition of inhibitor increases the values of $R_{ct}$ and reduces the $C_{dl}$. The decrease in $C_{dl}$ is attributed to the increase in thickness of the electronic double layer (Hosseini et al., 2007). The increase in $R_{ct}$ value is due to the formation of a protective film on the metal/solution interface (Bentiss et al., 2000; Murlidharan et al., 1995). These observations suggest that PPT molecules function by adsorption at the metal surface thereby causing the decrease in $C_{dl}$ values and increase in $R_{ct}$ values. The data obtained from the EIS technique are in good agreement with those obtained from potentiodynamic polarization and mass loss methods.

## 4. Conclusion

From the above results and discussion, the following conclusions are drawn: PPT inhibits the corrosion of Armco iron in 1 M $H_2SO_4$. The inhibition efficiency increases with the inhibitor concentration, but decreases slightly with the temperature.

- PPT acts as a mixed-type inhibitor.
- The adsorption of PPT on the iron surface from 1.0 M $H_2SO_4$ obeys a Langmuir adsorption isotherm. The adsorption process is a spontaneous and endothermic process.
- The kinetic and thermodynamic parameters of corrosion and adsorption processes are determined.
- The results obtained from weight loss, potentiodynamic polarization and impedance spectroscopy are in good agreement.

## References


Abboud, Y., Abourriche, A., Saffaj, T., Berrada, M., Charrouf, M., Bennamara, A., Hannache, H., 2009. Desalination 237, 175.

Ahamad, I., Prasad, R., Quraishi, M.A., 2010. Corros. Sci. 52, 1472.

Akiyama, A., Nobe, K., 1970. J. Electrochem. Soc. 17, 999.

Amar, H., Benzakour, J., Derja, A., Villemin, D., Moreau, B., Braisaz, T., Tounsi, A., 2008. Corros. Sci. 50, 124.

Amar, H., Benzakour, J., Derja, A., Villemin, D., Moreau, B., 2003. J. Electroanal. Chem. 558, 131.

Ashassi-Sorkhabi, H., Nabavi-Amri, S.A., 2000. Acta Chim. Slov. 47, 587.

Ateya, B.G., El-Anadouli, B.E., El-Nizamy, F.M., 1984. Corros. Sci. 24, 509.

Awad, H.S., Turgoose, S., 2004. Corrosion 60, 1168.

Awad, H.S., 2005. Anti-Corros. Methods Mater. 52, 22.

Ayers, R.C., Hackerman, N., 1963. J. Electrochem. Soc. 110, 507.

Bentiss, F., Traisnel, M., Lagrenee, M., 2000. Corros. Sci. 42, 127.

Benabdellah, M., Tounsi, A., Khaled, K.F., Hammouti, B., 2011. Arab. J. Chem. 4, 17.

Bouklah, M., Hammouti, B., Lagrenee, M., Bentiss, F., 2006. Corros. Sci. 48, 2831.

Cheng, S., Chen, S., Liu, T., Chang, X., Yin, Y., 2007. Mater. Lett. 61, 3279.

Choi, D.J., You, S.J., Kim, J.G., 2002. Mater. Sci. Eng. A 335, 228.

Ebenso, E.E., 2002. Mater. Chem. Phys. 71, 62.

Elayyachy, M., El Idrissi, A., Hammouti, B., 2006. Corros. Sci. 48, 2470.

El-Etre, A.Y., 2003. Corros. Sci. 45, 2485.

El-Naggar, M.M., 2007. Corros. Sci. 49, 2226.

Fang, J.L., Li, Y., Ye, X.R., Wang, Z.W., Liu, Q., 1993. Corrosion 49, 266.

Gonzalez, Y., Lafont, M.C., Pebere, N., Moran, F., 1996. J. Appl. Electrochem. 26, 1259.

Gomma, G.K., 1998. Mater. Chem. Phys. 55, 241.

Guan, N.M., Xueming, L., Fei, L., 2004. Mater. Chem. Phys. 86, 59.

Hackerman, N., 1962. Corrosion 18, 332.

Hackerman, N., Sudbury, J.D., 1950. J. Electrochem. Soc. 94, 4.

Herrag, L., Hammouti, B., Elkadiri, S., Aouniti, A., Jama, C., Vezin, H., Bentiss, F., 2010. Corros. Sci. 52, 3042.

Hosseini, M.G., Ehteshamzadeh, M., Shahrabi, T., 2007. Electrochem. Acta 52, 3680.

Hosseini, S.M.A., Azimi, A., 2009. Corros. Sci. 51, 728.

Jaworska, J., Genderen-Takken, H.V., Hanstveit, A., Plassche, E., Feijtel, T., 2002. Chemosphere 47, 655.

Laamari, R., Benzakour, J., Berrekhis, F., Abouelfida, A., Derja, A., Villemin, D., 2011a. Arab. J. Chem. 4, 271.

Laamari, R., Benzakour, J., Berrekhis, F., Derja, A., Villemin, D., 2016. Arab. J. Chem. 9, S245.

Laamari, R., Benzakour, J., Berrekhis, F., Derja, A., Villemin, 2010. Les Technologies de Laboratoire 5, 1.

Laamari, M.R., Derja, A., Benzakour, J., Berraho, M., 2001. Ann. Ch. Sci. Mat. 26, 117.

Laamari, M.R., Derja, A., Benzakour, J., Berraho, M., 2004. Elec. Anal. Chem. 569, 1.

Lebrini, M., Bentiss, F., Vezin, H., Lagrenee, M., 2006. Corros. Sci. 48, 1291.

Li, X., Mu, G., 2005. Appl. Surf. Sci. 252, 1254.

Martinez, S., Mansfeld-Hukovic, M., 2003. J. Appl. Electrochem. 33, 1137.

Mernari, B., Elattari, H., Traisnel, M., Bentiss, F., Legrenee, M., 1998. Corros. Sci. 40, 391.

Morad, M.S., 2008. Corros. Sci. 50, 436.

Morad, M.S., Kamal El-Dean, A.M., 2006. Corros. Sci. 48, 3398.

Murlidharan, S., Phani, K.L.N., Pitchumani, S., Ravichandran, S., 1995. J. Electrochem. Soc. 142, 1478.

Noor, E.A., Al-Moubaraki, A.H., 2009. Corros. Sci. 51, 868.

Obot, I.B., Obi-Egbedi, N.O., 2010. Corros. Sci. 52, 198.

Obot, I.B., Obi-Egbedi, N.O., 2008. Colloids Surf. A: Physicochem. Eng. Asp. 330, 207.

Onuchukwu, A.I., 1988. Mater. Chem. Phys. 20, 323.

Popova, A., Sokolova, E., Raicheva, S., Christov, M., 2003. Corros. Sci. 45, 33.

Schmitt, G., 1984. Br. Corros. J. 19, 165.

Shukla, S.K., Quraishi, M.A., 2009. Corros. Sci. 51, 1007.

Shih, H., Mansfeld, H., 1989. Corros. Sci. 29, 1235.

Singh, A.K., Quraishi, M.A., 2010. Corros. Sci. 52, 152.

Solomon, M.M., Umoren, S.A., Udosoro, I.I., Udoh, A.P., 2010. Corros. Sci. 52, 1317.

Szauer, T., Brandt, A., 1981. Electrochim. Acta 26, 1209.

Telegdi, J., Shaglouf, M.M., Shaban, A., Karman, F.H., Betroti, I., Mohai, M., Kalman, E., 2001. Electrochim. Acta 46, 3791.

Trachli, B., Keddam, M., Takenouti, H., Srhiri, A., 2002. Prog. Org. Coat. 44, 17.

Umoren, S.A., Ebenso, E.E., 2007. Mater. Chem. Phys. 106, 387.